



HAL
open science

Isotope removal experiment in JET-ILW in view of T-removal after the 2nd DT campaign at JET

T Wauters, D Matveev, D Douai, J Banks, R Buckingham, I S Carvalho, E de
la Cal, E Delabie, T Dittmar, J Gaspar, et al.

► **To cite this version:**

T Wauters, D Matveev, D Douai, J Banks, R Buckingham, et al.. Isotope removal experiment in JET-ILW in view of T-removal after the 2nd DT campaign at JET. *Physica Scripta*, 2022, 97 (4), pp.044001. 10.1088/1402-4896/ac5856 . hal-04029646

HAL Id: hal-04029646

<https://amu.hal.science/hal-04029646>

Submitted on 15 Mar 2023

HAL is a multi-disciplinary open access archive for the deposit and dissemination of scientific research documents, whether they are published or not. The documents may come from teaching and research institutions in France or abroad, or from public or private research centers.

L'archive ouverte pluridisciplinaire **HAL**, est destinée au dépôt et à la diffusion de documents scientifiques de niveau recherche, publiés ou non, émanant des établissements d'enseignement et de recherche français ou étrangers, des laboratoires publics ou privés.

Isotope removal experiment in JET-ILW in view of T-removal after the 2nd DT campaign at JET

T. Wauters¹, D. Matveev², D. Douai³, J. Banks⁴, R Buckingham⁴, I. S. Carvalho⁵, E. de la Cal⁶, E. Delabie⁷, T. Dittmar², J. Gaspar⁸, A. Huber², I. Jepu⁹, J. Karhunen¹⁰, S. Knipe⁴, M. Maslov⁴, A. Meigs⁴, I. Monakhov⁴, V. S. Neverov¹¹, C. Noble⁴, G. Papadopoulos⁴, E. Pawelec¹², S. Romanelli⁴, A. Shaw⁴, H. Sheikh⁴, S. Silburn⁴, A. Widdowson⁴, P. Abreu⁵, S. Aleiferis¹³, J. Bernardo⁵, D. Borodin², S. Brezinsek², J. Buermans¹, P. Card⁴, P. Carvalho⁵, K. Crombe¹, S. Dalley⁴, L. Dittrich¹⁴, C. Elsmore⁴, M. Groth¹⁵, S. Hacquin³, R. Henriques⁵, V. Huber², P. Jacquet⁴, X. Jiang², G. Jones⁴, D. Keeling⁴, D. Kinna⁴, K. Kirov⁴, M. Kovari⁴, E. Kowalska-Strzeciwiłk¹⁶, A.B. Kukushkin¹¹, H. Kumpulainen¹⁵, E. Litherland-Smith⁴, P. Lomas⁴, T. Loarer³, C. Lowry⁴, A. Manzanares¹⁷, A. Patel⁴, A. Peacock⁴, P. Petersson¹⁴, N. Petrella⁴, R. A. Pitts¹⁸, J. Romazanov², M. Rubel¹⁵, P. Siren¹⁷, T. Smart⁴, E. R. Solano⁶, Ž. Štancar^{4,19}, J. Varje¹⁵, A. Whitehead⁴, S. Wiesen², M. Zerbini²⁰, M. Zlobinski² and JET Contributors[†]

¹ Laboratory for Plasma Physics LPP-ERM/KMS, B-1000 Brussels, Belgium

² Forschungszentrum Jülich GmbH, Institut für Energie- und Klimaforschung, Plasmaphysik, 52425 Jülich, Germany

³ CEA, IRFM, F-13108 Saint Paul Lez Durance, France

⁴ United Kingdom Atomic Energy Authority, Culham Science Centre, Abingdon, Oxon, OX14 3DB, UK

⁵ Instituto de Plasmas e Fusão Nuclear, Instituto Superior Técnico, Universidade de Lisboa, 1049-001 Lisboa, Portugal

⁶ Laboratorio Nacional de Fusión, CIEMAT, Madrid, Spain

⁷ Oak Ridge National Laboratory, Oak Ridge, TN 37831, TN, United States of America

⁸ Aix-Marseille University, CNRS, IUSTI, UMR 7343, 13013 Marseille, France

⁹ The National Institute for Laser, Plasma and Radiation Physics, Magurele-Bucharest, Romania

¹⁰ University of Helsinki, PO Box 43, FI-00014 University of Helsinki, Finland

¹¹ NRC Kurchatov Institute, 1 Kurchatov Square, Moscow 123182, Russian Federation

¹² Institute of Physics, Opole University, Oleska 48, 45-052 Opole, Poland

¹³ NCSR 'Demokritos' 153 10, Agia Paraskevi Attikis, Greece

¹⁴ KTH Royal Institute of Technology, EECS, Dept. Fusion Plasma Physics, 100 44 Stockholm, Sweden

¹⁵ Aalto University, PO Box 14100, FIN-00076 Aalto, Finland

¹⁶ Institute of Plasma Physics and Laser Microfusion, Hery 23, 01-497 Warsaw, Poland

¹⁷ Universidad Complutense de Madrid, Madrid, Spain

¹⁸ ITER Organization, Route de Vinon-sur-Verdon, CS 90 046, 13067 St Paul Lez Durance Cedex, France

¹⁹ Slovenian Fusion Association (SFA), Jozef Stefan Institute, Jamova 39, SI-1000 Ljubljana, Slovenia

²⁰ Dip.to Fusione e Tecnologia per la Sicurezza Nucleare, ENEA C. R. Frascati, via E. Fermi 45, 00044 Frascati (Roma), Italy

[†] See the author list of 'Overview of JET results for optimising ITER operation' by J. Mailloux et al. to be published in Nuclear Fusion Special issue: Overview and Summary Papers from the 28th Fusion Energy Conference (Nice, France, 10-15 May 2021)

E-mail: tom.wauters@iter.org

Received xxxxxx

Accepted for publication xxxxxx

Published xxxxxx

Abstract

A sequence of fuel recovery methods was tested in JET, equipped with the ITER-like beryllium main chamber wall and tungsten divertor, to reduce the plasma deuterium concentration to less than 1% in preparation for operation with tritium. This was also a key activity with regard to refining the clean-up strategy to be implemented at the end of the 2nd DT campaign in JET (DTE2) and to assess the tools that are envisaged to mitigate the tritium inventory build-up in ITER. The sequence began with 4 days of main chamber baking at 320°C, followed by a further 4 days in which Ion Cyclotron Wall Conditioning (ICWC) and Glow Discharge Conditioning (GDC) were applied with hydrogen fuelling, still at 320°C, followed by more ICWC while the vessel cooled gradually from 320°C to 225°C on the 4th day. While baking alone is very efficient at recovering fuel from the main chamber, the ICWC and GDC sessions at 320°C still removed slightly higher amounts of fuel than found previously in isotopic changeover experiments at 200°C in JET. Finally, GDC and ICWC are found to have similar removal efficiency per unit of discharge energy. The baking week with ICWC and GDC was followed by plasma discharges to remove deposited fuel from the divertor. Raising the inner divertor strike point up to the uppermost accessible point allowed local heating of the surfaces to at least 800°C for the duration of this discharge configuration (typically 18 s), according to infra-red thermography measurements. In laboratory thermal desorption measurements, maintaining this temperature level for several minutes depletes thick co-deposit samples of fuel. The fuel removal by 14 diverted plasma discharges is analysed, of which 9, for 160 s in total, with raised inner strike point. The initial D content in these discharges started at the low value of 3-5%, due to the preceding baking and conditioning sequence, and reduced further to 1%, depending on the applied configuration, thus meeting the experimental target.

Keywords: Tritium, Inventory, JET, DTE2, ITER, Wall conditioning

1. Introduction

Since the installation of the beryllium (Be) main chamber wall and tungsten (W) divertor, the JET tokamak is uniquely equipped to study material erosion and migration in the vessel along with the retention and removal of fuel in the most ITER-relevant conditions [1]. Campaign-averaged information on long-term fuel retention and material migration processes is systematically obtained, *ex-situ*, by post-mortem analysis of components removed from the JET vessel after operation campaigns [2]–[4]. Such analysis after the third ITER-like wall (ILW) campaign (ILW-3, executed in 2015-2016) confirmed the previous trends found for ILW-1 and ILW-2: fuel retention in JET is dominated by co-deposition with Be, for which the thickest deposits, up to a few tens of μm , are found on Tiles 0 and 1 (see section 4) of the inner divertor [5]. For the ILW-3 campaign, this location retains 46.5% of all the accumulated fuel while 13.4% is found at the outer divertor, 14.3% on the main chamber limiters and upper dump plates, 10.5% on recessed areas of the main chamber and 12.4% in main chamber gaps such as castellation grooves on plasma-facing components (PFC). The global retention rate for ILW-3, normalised to the divertor plasma time, is 6.3×10^{18} D/s [2] while gas balance analysis, assessing the fuel inventory *in situ* and on shorter timescales, estimates $0.2 - 1.5 \times 10^{20}$ D/s [3], [6], [7] with a spread that is explained by the strong dependence of retention on the discharge scenarios and the chosen outgassing duration. The same effect, namely the dependence of the dynamic and long-term retention reservoirs on the considered outgassing time after plasma operation [8], explains the difference between the results of *ex-situ* and *in-situ* retention analysis at JET.

Fuel recovery techniques, which are the topic of this paper, target the long-term retention. Tokamaks working with tritium (T) may have several reasons to apply such techniques. They are essential to the clean-up strategy to be implemented at the end of the 2nd DT campaign in JET (DTE2). Moreover, the ongoing JET campaigns, operating with deuterium (D), T and D-T mixtures have strict limits on the number of 14 MeV neutrons produced by fusion reactions in each of the campaign phases. These are set so as not to unnecessarily consume the total neutron budget of the facility set by vessel activation limits [9]. This requires that the residual D content in the plasma be reduced to 1% from the start of the T-phase, and similarly for the residual T content in the D-phase following D-T operation. The JET DT safety case limits the potentially releasable T inventory (by loss of vacuum) at any given time to 15 g [10], and assumes that the long-term T retention is at most 4 g. In

ITER, the maximum allowed retention in the in-vessel components is set at 700 g. At a JET-like retention fraction of the injected fuel of 0.14-0.19% [5], without recovery methods, ITER could potentially reach this limit already within the first fusion power operation (FPO) campaigns [9]. The actual retention fraction is sensitively dependent on wall surface temperatures and incident particle fluences/energies, which may be very different in ITER [11]. For these reasons it is essential that the fuel recovery techniques available to JET and ITER be tested and characterized as thoroughly as possible.

The fuel outgassing efficiency from PFCs exposed in JET-ILW has been studied at ITER-relevant baking temperatures, suggesting that fuel removal from thick deposits will be difficult [12], [13]. Only 13% of fuel could be removed from 40 μm thick co-deposit layers on the W coated CFC divertor tiles by 15 hours of baking at 350°C [12]. The JET ILW-1 campaign deposited such layers across the entire campaign, whereas this may occur in only a few days of ITER operation under $Q = 10$, burning plasma conditions [13]. Removal of implanted fuel from the JET Be main chamber samples in the deposit-free erosion zones of limiter tiles on the midplane by baking at 240°C was even less efficient [12]. From these and similar studies, it is known that all fuel (whether or not in co-deposited layers) is recovered when the surfaces are heated to temperatures of at least 800°C for several minutes [12]–[14].

The ITER wall conditioning and fuel removal techniques include baking, glow discharge cleaning (GDC) and RF discharges without plasma current, both in the ion cyclotron and electron cyclotron range of frequencies (ICWC and ECWC). JET does not have an electron cyclotron heating system, but routinely uses limiter and diverted plasmas with nested magnetic flux surfaces for cleaning purposes. Moreover, its flexible configuration allows it to place the inner divertor strike point on top of Tile 1, high up on the inner vertical target, so that thermal plasma can be used to heat the local deposits.

2. Experiment strategy

The JET experiment presented here combines the available fuel removal techniques to bring the D concentration in hydrogen (H) plasma down to 1% before the start of the T operations campaign. The rationale behind the experimental strategy is that fuel removal is accelerated at higher temperatures, but that baking alone, at 320°C for the first wall (FW) and about 200°C for the upper part of the lower divertor, is insufficient to exhaust the inventory completely. Figure 1 shows the

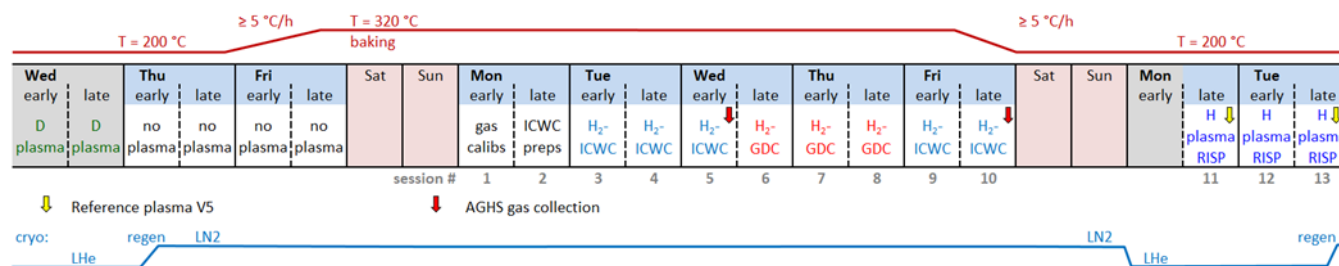


Figure 1: Timeline of the isotopic exchange experiment indicating the baking duration, the ICWC, GDC and diverted plasma operation sessions, the cooling of the divertor cryopanels, either by liquid helium or nitrogen, the collection of pumped gas at the Active Gas Handling System (AGHS) and reference pulses in the V5 divertor configuration. “Early” and “Late” refer to the two operational shifts which JET runs on each experimental day.

timeline of the experiment. One day after the end of the D operations phase, the divertor cryopumps were warmed-up to liquid nitrogen temperature and the vessel temperature was ramped from the 200°C temperature used for normal operations, up to 320°C at a rate of about 5°C per hour. During this time, the divertor maintains the cooling water flow at room temperature to protect the in-vessel divertor coils. This results in a temperature gradient over the divertor tiles, where Tiles 0 and 1 are at most at 150-200°C, the vertical tiles 3 and 7 at 100-150°C and the bottom tiles 4 and 6 at least at 50°C, based on thermocouple trends. The locations of these tiles are indicated in Fig. 3c. The steady baking temperature is maintained for 7 days, in the second half of which, cycles of ICWC and GDC in H are performed. Two days after completing the baking procedure, the cryopanels were cooled to liquid helium temperature in preparation for diverted cleaning plasmas with raised inner strike points, aiming at heating the Tile 1 surface layers.

Sub-divertor residual and optical gas analysers (RGA and OGA) [15], [16] are used to quantify the isotopic content in the outgassed molecules. The data is compared to mass spectrometry data from the midplane pumping ducts, H_α high-resolution spectroscopy of the main chamber and divertor [17], as well as the quantifications and chromatography of gas collected by the pumps [18]. The temperatures of the plasma-facing surfaces are monitored by infra-red (IR) thermography [19] and subsurface thermocouples [20].

3. Baking at 320°C with ICWC and GDC

Figure 2 shows the vessel temperature and the partial pressures of HD and D₂ taken in the midplane pumping ducts during the baking week. As the temperature of the vessel rises, thermal desorption of D tracks the temperature waveform, as can be seen in the RGA traces. During the first 24 hours following the achievement of the 320°C plateau, the outgassing pressure decays by a factor of ~ 3 . Beyond this point, it decreases more slowly, typical of the often-observed power law outgassing dependency

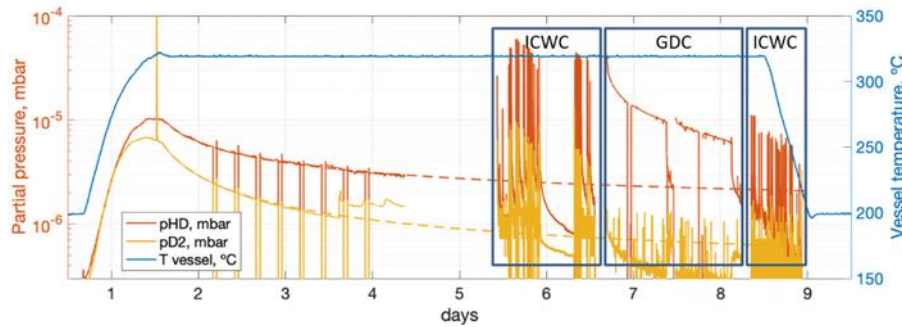


Figure 2: Partial pressures of HD and D₂ (left axis) and vessel temperature (right axis) throughout the baking week.

[8]. The discontinuities in the pressure traces at time intervals of 6 hours are due to background measurements during which the RGAs are temporarily isolated from the torus. A jump in the D₂ pressure is visible at 3.6 days, corresponding to a slow leak through gas injectors that have been prepared to perform gas puffs for RGA and OGA calibrations. These calibrations took place around day 5 on the graph, and the associated pressure data has been removed for clarity.

Hydrogen ICWC was applied in two phases, 27 pulses before GDC and 25 pulses after GDC, as also seen in Fig. 2. The pressure peaks are the result of the post-discharge release of gas from the PFCs, while the steady discharge pressure is controlled at 1.8×10^{-5} mbar. These ICWC discharges, targeting the replacement of near surface retained D atoms by isotopic exchange with H, were produced by coupling 100-250 kW of power in the ion cyclotron range of frequencies (ICRF), at 29 MHz, in the presence of a toroidal field in most cases of 1.9 T and a barrel shaped vertical field of 15 mT on axis [21]. A tangential camera view of an ICWC plasma in JET is shown in Fig. 3a to emphasize the uniformity of the RF glow with apparent strongest interaction at the inboard and outboard limiters. The experiment applied mostly 17 s long ICWC pulses, repeated every 15-20 minutes to allow for diagnostic post-processing and machine preparations for these JET pulse-based discharges (required because the toroidal field is not permanently on in JET). It is important to note that ITER (where the toroidal field will be permanently energized during operational campaigns) will apply RF conditioning programmes as sequences of multiple discharges, similar to the so-called pulse trains in W7-X [22]. This will allow higher repetition rates and duty cycle optimisation to minimise the re-deposition of wall released isotopes.

The GDC on JET in the experiments reported here was performed with 3 anodes at 2.5-4 A and 205-275 V, delivering 2.4 kW of DC power to the plasma, without magnetic field, at a steady neutral pressure of 3.1×10^{-3} mbar. A camera view of a GDC plasma is shown in Fig. 3b, illustrating the uniformity of the discharge and the anode location at the top of the vessel where the bright anode glow is seen. Hydrogen GDC was applied in two continuous procedures of ~ 17 hours and ~ 16 hours respectively. A 1 hour-long discontinuity is visible in Fig. 2 about halfway through each glow phase when the background neutral gas at the midplane RGA was monitored. The glows are separated by 2 hours, as seen in the outgassing traces of Fig. 2 starting at 7.7 days, to provide better understanding of the D removal process. The first glow displays a rapid decrease of the outgassing by a factor of 3 in the first 6 hours, with thereafter a slower trend, typical of the power law outgassing dependency referred to earlier. The second glow does not show this feature and continues the outgassing rate approximately at the level where it was interrupted. Thus, the accessible isotope reservoir does not seem to be significantly repopulated by diffusion from deeper layers in the dwell time between the two glows, even at baking temperatures. Therefore, the accessible reservoir may be rather determined by the extent of the transient loading of the surfaces by isotopes provided via the conditioning discharge and the mechanism of isotopic exchange. Since the JET GDC system does not allow the glow to be initiated at operating pressure, unlike in e.g. ASDEX Upgrade [23], it is difficult to investigate this further in JET, nor is it possible to implement a more meaningful discharge cycle which minimises re-deposition or material sputtering.

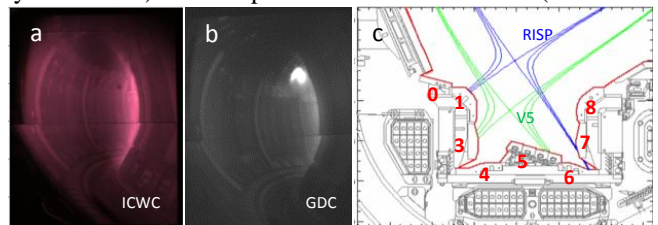


Figure 3: Tangential camera images of typical ICWC (a) and GDC (b) discharges in JET. Right (c): Magnetic flux surfaces at the divertor for the Raised Inner Strike Point (RISP) and V5 configuration with numbering of the divertor tiles in red.

3.1 Gas balance

Baking, from the start of the temperature rise to the first ICWC discharge, corresponding to 5.4 days in Fig. 2, removed 2.9×10^{23} D atoms from the vessel. This amount is an average of partial pressure measurements with 2 midplane and 4 sub-divertor RGAs, and estimated extrapolation of the pressures along the outgassing trend described by the dashed lines in Fig. 2. Extrapolating the trend to the last ICWC discharge at the end of the baking week, corresponding to 9 days in Fig. 2, predicts that an additional 1.2×10^{23} D atoms could have been removed by continued baking without ICWC or GDC. This latter number is probably overestimated and should be used with caution given the uncertainty of the extrapolation.

The removal in the ICWC sessions is obtained by collecting and analysing all the pumped gas, starting from the first ICWC discharge and ending with 1.5 hours of outgassing after the last ICWC discharge in each of the two ICWC phases. The first phase (Sessions 3-5 in Fig. 1) with an energy throughput of 85.7 MJ performed over 27.9 hours removed 7.3×10^{22} D atoms while the second (Sessions 9-10 in Fig. 1) removed 1.7×10^{22} D for an energy throughput of 57.4 MJ over 13.9 hours (recall that the ICWC is only applied in short pulses separated by 15-20 minute intervals and that the usual outgassing occurs between each set of pulses). For completeness, the removed amount estimated from 2 sub-divertor RGAs is given, each combining the pulse-based recordings (not available for the midplane RGAs) with a time resolution of 0.33 seconds per sample and per mass channel, and the continuous data measured in-between pulses at a lower time resolution. Since deconvolution of this RGA data becomes increasingly unreliable at decreasing isotopic concentration, the removal is underestimated by a factor of ~ 2 .

Similarly, since the deconvolution of the sub-divertor RGAs became unreliable in the last 16 hours of the procedure with increasingly lower pressures, the gas balance for the GDC sessions is obtained from the 2 midplane RGAs only. An estimated 1.3×10^{23} D atoms were removed by the 33 hours of GDC, corresponding to a total energy input of 285 MJ.

Applying GDC and ICWC in addition to baking yields a two-fold gain compared to baking alone. ICWC applied after an extensive GDC procedure still removes a significant quantity of D atoms, but less than the first ICWC sessions. From this it is concluded that both GDC and ICWC share to a large extent their plasma-wall interaction areas.

ICWC and GDC may be considered to have at best a uniform wetting of the plasma-facing surfaces (see Fig. 3 a and b). The first field lines intersecting components during ICWC plasmas, such as main chamber limiters, carry most of the ion flux, while the recessed areas including gaps such as castellations and recessed areas on the main wall are conditioned by a flux of neutral atoms [24], [25]. Gas balance analysis, which includes the removal trends discussed in the next sections, integrates the removal from all these areas. *In-situ* diagnostic techniques, such as Laser Induced Desorption with detection by Quadrupole Mass Spectrometry (LID-QMS), currently being prepared for JET [26] and ITER, are required to assess the removal from a particular location. The removed amounts throughout the baking week, estimated by gas balance analysis, are a significant fraction of the inventory based on post-mortem analysis (43%), as detailed in [5]. However, the analysis of the extracted material samples is completed 1-2 years after their last plasma exposure in JET, while outgassing continues throughout this period. Similarly, only local, *in-situ* measurements could provide some estimate of the inventory at the start of this experiment, built up during plasma exposure and slowly, but continuously depleted by outgassing during the campaign period (running over 1-2 years).

3.2 Gain of combining ICWC and GDC with baking

Earlier work reported a removal of 10^{23} atoms by 1.26 hours of GDC at 200°C in JET-ILW [27]. The same duration in the present experiment at 320°C removed 1.2×10^{22} D atoms (where the 1.26 hours is counted from the establishment of the GDC discharge). This almost an order of magnitude difference is due to the depletion of the surface of D by the several days of baking and the ICWC sessions which preceded the GDC. This clearly illustrates that substantially more fuel can be recovered by extending the conditioning procedure; the accessible reservoir depends on the conditioning duration. Thus, although the first ~ 1.5 hours of GDC in the current experiment at 320°C removed less than the older reported result, the total removal over the 33 glow hours here did exceed that obtained at 200°C despite the preceding surface depletion.

In addition to duration, the accessible reservoir for isotope exchange depends on the surface temperature. Comparison of the cumulated removal by ICWC capped at an energy throughput of 85 MJ in the first ICWC phase before GDC, and previous ICWC work at 200°C in JET-ILW [28], gives 7.3×10^{22} and 5.6×10^{22} atoms, respectively. Thus, ICWC at 320°C

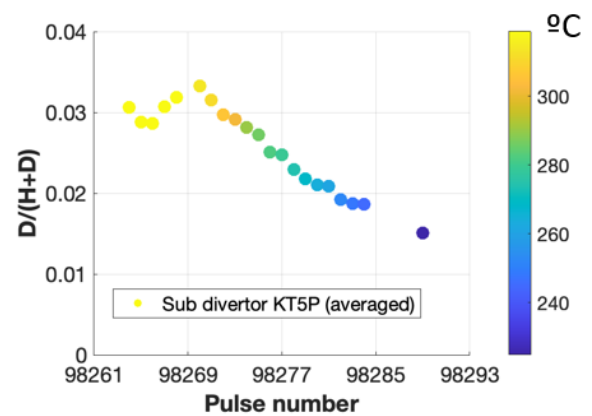


Figure 4: D content from sub divertor OGA in ICWC discharges of Sessions 9-10 (Fig. 1) and vessel temperature.

appears to be more effective than at normal JET operating temperature, even despite the prior baking days. The same energy throughput in GDC removed 6.2×10^{22} atoms, only slightly lower, despite the preceding desaturation by ICWC.

The vessel temperature was ramped down from 320°C to 225°C during the last ICWC phase (Sessions 9-10 in Fig. 1). While the D content is fairly constant at first in the ICWC discharges, still at constant vessel temperature, it steadily decreases with the decreasing temperature, as shown in Fig. 4. This again indicates a reduced removal efficiency at a lower surface temperature, which is of particular concern for ITER, where ICWC will be used while the PFCs are cooled to 70°C (the ITER ion cyclotron resonance heating (ICRH) antennas cannot be used at FW baking temperature). Dedicated isotope exchange experiments which investigate the temperature dependence are therefore required, both in JET, where ICWC may be operated at 110°C, approaching the ITER-relevant surface temperature, and in dedicated facilities such as TOMAS [29] where samples can be exposed to ICWC and GDC at controlled temperatures.

3.3 Total removal and discharge energy throughput

Figure 5, adapted from [21], shows cumulated removal tendencies for earlier ICWC experiments in JET-ILW, with the present ICWC (purple asterisk) and GDC (continuous green line) experiment added. Plotted as function of the cumulated coupled ICRF energy, these experiments followed a E^n power law envelope curve with exponent $n = 0.5$ for the integrated removal. A curve with this same exponent has been added (dashed line) to illustrate the similarity between the ICWC and GDC energy efficiency, expressing the total removal as a function of the cumulated energy throughput. Here it is considered that the input power is a measure for the ion flux in GDC [30], and neutral flux in ICWC [31], to the main chamber surfaces. It is important to note that the trend (dashed) line shows no saturation even though the integral of the coupled ICRF and GDC power exceeds the previous experiments by a factor of 3. This indicates that significantly more atoms may still be removed by extending the conditioning procedure, which is typical for the power law dependency. By extending the procedure, the accessible reservoir increases due to an increased discharge energy throughput.

If the power throughput is indeed the rate determining factor, the energy consumption of GDC and ICWC needs to be mapped to the wall-clock time. In a tokamak with superconducting coils (such as ITER, but unlike JET), the equivalent discharge energy of 33 hours of GDC at 2.4 kW can be applied using ICWC at 250 kW of coupled power within a period of 3 hours at a 10% duty cycle. This means that fuel removal by ICWC may be 10 times faster than GDC. While this number is striking, the duty cycle must be considered in more detail, which may be performed *in silico* by reaction diffusion modelling of isotopic exchange. Indeed, outgassing from PFCs is a slow process that continues during the dwell time between the ICWC pulses.

4. Diverted plasma with raised inner strike point

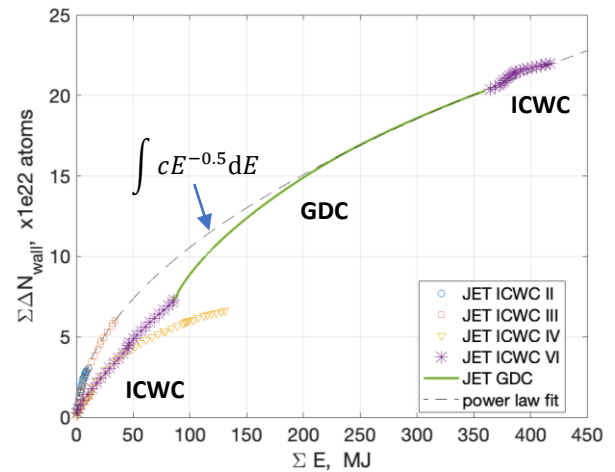
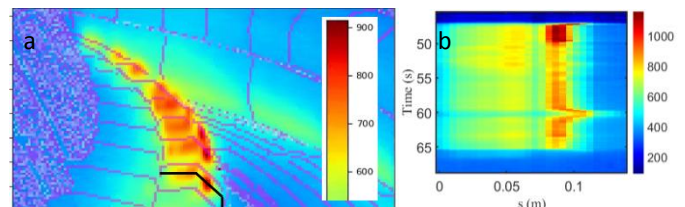


Figure 5: Total removal vs. discharge energy throughput for earlier ICWC experiments on JET-ILW at 25MHz (II, III & IV [21]), and the present combined ICWC (VI) and GDC experiment. The dashed line is a possible envelope curve for the total removal in case of a previously observed $E^{0.5}$ removal dependency [21]



Post-mortem analysis of JET PFCs showed that 46.5% of the retained fuel is deposited along with Be on the upper part of the inner divertor [5]. In order to deplete these surface layers from fuel by thermal outgassing alone, they must be heated above 800 °C for several minutes, based on TDS spectra [14]. To achieve these temperature conditions locally, *in situ*, a diverted plasma scenario was developed with a stationary phase of 18 s in which the inner strike point is raised up to the uppermost accessible point on Tile 1, where the thickest deposits reside. The resulting raised inner strike point (RISP) configuration is illustrated by the blue flux surfaces in Fig. 3c. For comparison, the green flux surfaces show the typical JET V5 configuration. Following the week of high temperature baking, a total of 9, main chamber hydrogen fuelled RISP discharges have been performed at the usual 200°C vessel operating temperature. These L-mode discharges at 1.8 T, 1.7 MA and 2 to 4.5 MW of ICRH power at 51 MHz reached a central line averaged density of $2.3 \times 10^{19} \text{ m}^{-3}$, with high recycling conditions at the inner strike point characterised by a peak temperature of 5-10 eV and density of $1.5 \times 10^{20} \text{ m}^{-3}$ at the target.

In total 2.4×10^{22} D atoms have been removed in 14 diverted plasma discharges, including the 9 RISP pulses, as obtained from volumetric and chromatography analysis of the pumped gas. The removed amount represents 12.5% of the long term retention at Tiles 0 and 1 found in post-mortem analysis. Comparing these numbers ignores, however (i) the possible depletion of the divertor deposits during the baking week with ICWC and GDC, (ii) the removal from other areas during the diverted discharges, (iii) the re-deposition of fuel removed from Tiles 0 and 1 during the discharge and (iv) the continuous slow outgassing of these layers before their *ex situ* analysis as described in Section 3. This again emphasises the importance of *in situ* quantification of the fuel content in the divertor PFCs.

The limited thermal conductivity of the deposits to the substrate layer helps in heating them during the plasma exposure [32]. Infra-red images of the divertor (Fig. 6) show that the enhanced heat flux brought the Tile 1 surface temperature to the target value of 800°C and above, for the duration of the discharges. At the same time, it is observed that the heating is non-uniform, both in the poloidal and toroidal directions. The sharp temperature variations seen at the end of the discharge and during a strike point sweep applied around 60 s in Fig. 6b, are consistent with the assumption of resistive surface deposits. Thermocouple data (not shown here) indicate only a small ratcheting of the tile base temperature of about 50°C throughout the subsequent RISP pulses. While heating of the bulk material of about 100°C per pulse was observed, reaching a maximum temperature of about 200°C overall, the pulse repetition rate was clearly too low to substantially increase the base temperature.

RISP reaches high Tile 1 surface temperatures with modest input power. It appears to be challenging to reach such high surface temperatures with other plasma configurations. The standard V5 configuration (green flux surfaces in Fig. 3c) attains 500°C at Tile 1 thanks to a relatively small distance between the inner baffle and the separatrix (interestingly, in the present experiment, a Tile 1 surface temperature of about 450°C was reached in ICWC discharges where the fundamental resonance layer of the D minority was placed at the inner divertor). While these temperatures are insufficient for complete thermal outgassing of the layers, these vertical plasma configurations (which are the standard configurations used on ITER) may be considered as a means to limit the fuel content in the inner divertor layers through isotopic exchange, before subsequent deposits build up. The feasibility of plasma-induced removal from deposits as a potential means of T control in ITER was explored in [14], and needs to be investigated further, though the active cooling of PFCs in ITER may make it difficult to raise the surface temperatures significantly, especially far from the strike points where most of the deposits are expected to accumulate, unless their conductivity to the W divertor monoblocks is sufficiently low.

Figure 6: Divertor IR thermography illustrating the geometric (a) and temporal (b, 1D taken along black curve in a) pattern of the heating at the inner divertor, for a discharge with RISP (JPN98298, camera KL7-E8WB).

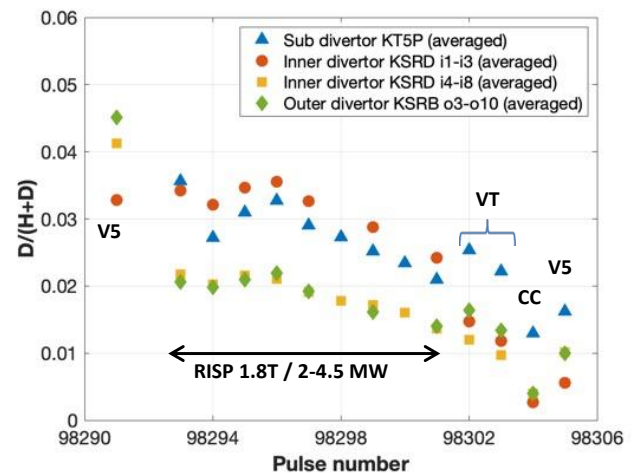


Figure 7 summarises the isotopic content in the diverted plasmas measured by the sub-divertor OGA and spatially-resolved H_α high-resolution spectroscopy. As a consequence of the preceding conditioning sequence, described in Section 3, the D content in a reference discharge with V5 configuration started at the low value of 3-5% in plasma. It subsequently decreased further to 1%, depending on the applied configuration, in the 14 discharges (including the 9 RISP pulses). This then meets the overall target of these inventory control experiments.

The spectroscopy measurements at the upper inner divertor (KSRD [17] channels i1-i3 in Fig. 7) consistently show a higher D content in the RISP discharges compared to other divertor locations, indicative of the locally stimulated thermal outgassing. While the difference between these measurements decreases from pulse to pulse, it can be seen that the change-over on Tile 1 is not yet complete on the last RISP pulse.

The isotopic content of the neutral gas in the sub-divertor, representative of the pumped gases, is consistently higher than the divertor spectroscopy measurements in non-RISP discharges, indicating that additional D fuel is released in these discharges from locations not accessible by RISP. Separately, it is recognised that the sensitivity limit for isotopic ratio measurements by the OGA is close to the resulting D content in H of 1-2%.

5. Conclusion

A sequence of fuel recovery schemes following a long deuterium plasma operation campaign was tested in JET to reduce the plasma D concentration to below 1%. The experiment aimed at refining the clean-up strategy to be implemented at the end of the JET DTE2 campaign and assessed tools that are envisaged to mitigate the tritium inventory build-up in ITER. The sequence in JET, equipped with the ITER-like beryllium main chamber wall and tungsten divertor, began with 4 days of baking removing 2.9×10^{23} D atoms, presumably from the main chamber surfaces. While the vacuum vessel is heated to 320°C in this procedure, the JET divertor continues to be cooled to protect in-vessel components, keeping the upper divertor surfaces below 150-200°C and still lower for surfaces lower down in the divertor. In the subsequent 4 days, (i) Ion Cyclotron Wall Conditioning (ICWC) and (ii) Glow Discharge Conditioning (GDC) were applied with hydrogen fuelling, still at 320°C, followed by (iii) hydrogen ICWC while the vessel cooled gradually from 320°C to 225°C on the 4th day. Gas balance analysis yields estimates of the removal at respectively (i) 7.3×10^{22} , (ii) 1.3×10^{23} and (iii) 1.7×10^{22} D atoms. While baking alone removed a significant amount of fuel, the subsequent ICWC and GDC sessions still removed slightly higher amounts than found previously in isotopic changeover experiments in JET with the vacuum vessel at 200°C.

The GDC procedure, consisting of two glows of 17 and 16 hours, separated by 2 hours for passive outgassing, found no evidence of temporarily increased D outgassing in the second GDC. The isotope flux from the conditioning plasma, rather than diffusion in the material, seems to be the process determining factor at the timescale of this experiment. The removal by GDC as a function of the coupled energy (285 MJ in total), continues approximately along the same power law fit for the removal by ICWC (85.7 MJ in total before and 57.4 MJ after GDC), indicating a comparable particle flow per unit of coupled energy and equivalent plasma-material interaction areas. A clear positive correlation between fuel removal and surface temperature is found in the ICWC pulses at different main chamber wall temperatures during the vessel cool down from 320°C to 225°C.

About half of the trapped fuel is co-deposited on the upper part of the lower divertor inner target, as evidenced by post-mortem analysis following previous JET-ILW campaigns [5]. Raising the inner divertor strike point onto Tile 1 in a specially designed scenario allowed these co-deposited layers to be locally heated above 800°C for the duration of the tokamak discharge. In total, 2.4×10^{22} D atoms were removed in 14 discharges, 9 of which (for an integral duration of 162 s) with raised inner strike point. The plasma D content in these discharges started at the low value of 3-5%, due to the preceding baking and conditioning sequence, and reduced further to 1% depending on the applied plasma configuration, thus meeting the overall target set for this fuel recovery experiment.

The amounts removed in this experiment approach the long-term inventory obtained by post-mortem analysis of material samples extracted from the JET PFCs (43% of the retention measured in [5]). To make this comparison quantitative requires a correction for the continuous slow outgassing of these samples before they are analysed *ex situ*. Since such a scaling over a long time period is inevitably inaccurate, *in situ* quantification of the in-vessel inventory content is very much needed.

Acknowledgements

This work has been carried out within the framework of the EUROfusion Consortium and has received funding from the Euratom research and training programme 2014-2018 and 2019-2020 under grant agreement No 633053. The views and opinions expressed herein do not necessarily reflect those of the European Commission, nor of the ITER Organization.

References

Figure 7: Isotopic content in diverted plasmas by sub-divertor OGA and spatially-resolved high-resolution H_α spectroscopy. The V5 and RISP divertor configurations are illustrated in Fig. 3c. The VT and CC configurations put the inner and outer strike points on the vertical targets (Tiles 3 and 7 in Fig. 3c) and lower corner tiles (Tiles 4 and 6 in Fig. 3c) respectively.

- [1] G. F. Matthews *et al.*, “Overview of the ITER-like wall project*,” *Phys. Scr.*, vol. 2007, no. T128, p. 137, Mar. 2007, doi: 10.1088/0031-8949/2007/T128/027.
- [2] J. Likonen *et al.*, “First results and surface analysis strategy for plasma-facing components after JET operation with the ITER-like wall,” *Phys. Scr.*, vol. T159, p. 014016, Apr. 2014, doi: 10.1088/0031-8949/2014/T159/014016.
- [3] K. Heinola *et al.*, “Fuel retention in JET ITER-Like Wall from post-mortem analysis,” *J. Nucl. Mater.*, vol. 463, pp. 961–965, Aug. 2015, doi: 10.1016/j.jnucmat.2014.12.098.
- [4] A. Widdowson *et al.*, “Overview of fuel inventory in JET with the ITER-like wall,” *Nucl. Fusion*, vol. 57, no. 8, Art. no. 8, Jul. 2017, doi: 10.1088/1741-4326/aa7475.
- [5] A. Widdowson, “Evaluation of tritium retention ...,” *Phys. Scripta*, 2021.
- [6] S. Brezinsek *et al.*, “Fuel retention studies with the ITER-Like Wall in JET,” *Nucl. Fusion*, vol. 53, no. 8, Art. no. 8, Jul. 2013, doi: 10.1088/0029-5515/53/8/083023.
- [7] T. Loarer *et al.*, “Plasma isotopic changeover experiments in JET under carbon and ITER-like wall conditions,” *Nucl. Fusion*, vol. 55, no. 4, Art. no. 4, Mar. 2015, doi: 10.1088/0029-5515/55/4/043021.
- [8] V. Philipps *et al.*, “Dynamic fuel retention and release under ITER like wall conditions in JET,” *J. Nucl. Mater.*, vol. 438, pp. S1067–S1071, Jul. 2013, doi: 10.1016/j.jnucmat.2013.01.234.
- [9] E. Joffrin *et al.*, “Overview of the JET preparation for deuterium–tritium operation with the ITER like-wall,” *Nucl. Fusion*, vol. 59, no. 11, p. 112021, Aug. 2019, doi: 10.1088/1741-4326/ab2276.
- [10] H. Boyer, D. Plummer, and J. Johnston, “JET Tokamak, preparation of a safety case for tritium operations,” *Fusion Eng. Des.*, vol. 109–111, pp. 1308–1312, Nov. 2016, doi: 10.1016/j.fusengdes.2015.12.037.
- [11] R. A. Pitts, “Progress in the understanding of plasma-wall interactions in support of the ITER Research Plan,” Jun. 2021, p. (paper I1-001). [Online]. Available: <http://ocs.ciemat.es/EPS2021ABS/pdf/I1.001.pdf>
- [12] K. Heinola *et al.*, “Long-term fuel retention and release in JET ITER-Like Wall at ITER-relevant baking temperatures,” *Nucl. Fusion*, vol. 57, no. 8, Art. no. 8, Jun. 2017, doi: 10.1088/1741-4326/aa747e.
- [13] G. De Temmerman *et al.*, “Efficiency of thermal outgassing for tritium retention measurement and removal in ITER,” *Nucl. Mater. Energy*, vol. 12, pp. 267–272, Aug. 2017, doi: 10.1016/j.nme.2016.10.016.
- [14] A. Založnik, R. P. Doerner, and G. De Temmerman, “Deuterium removal from beryllium co-deposits by simulated strike-point sweeping,” *Nucl. Mater. Energy*, vol. 24, p. 100750, Aug. 2020, doi: 10.1016/j.nme.2020.100750.
- [15] I. Jepu, “Subdivertor RGA and OGAs,” *Phys. Scripta*, 2021.
- [16] U. Kruezi *et al.*, “Neutral gas analysis for JET DT operation,” *J. Instrum.*, vol. 15, no. 01, pp. C01032–C01032, Jan. 2020, doi: 10.1088/1748-0221/15/01/C01032.
- [17] V. S. Neverov, A. B. Kukushkin, U. Kruezi, M. F. Stamp, and H. Wiesen, “Determination of isotope ratio in the divertor of JET-ILW by high-resolution Ha spectroscopy: H–D experiment and implications for D–T experiment,” *Nucl. Fusion*, vol. 59, no. 4, Art. no. 4, Feb. 2019, doi: 10.1088/1741-4326/ab0000.
- [18] S. G. Romanelli *et al.*, “Upgraded Analytical Gas Composition Technique in the Tritium Fuel Cycle of JET,” *Fusion Sci. Technol.*, vol. 71, no. 4, pp. 467–472, May 2017, doi: 10.1080/15361055.2017.1293432.
- [19] I. Balboa *et al.*, “Recent developments of in-vessel calibration of mid-IR cameras at JET,” *Rev. Sci. Instrum.*, vol. 87, no. 11, p. 11D419, Nov. 2016, doi: 10.1063/1.4960323.
- [20] C. Guillemaut *et al.*, “Main chamber wall plasma loads in JET-ITER-like wall at high radiated fraction,” *Nucl. Mater. Energy*, vol. 12, pp. 234–240, Aug. 2017, doi: 10.1016/j.nme.2017.02.010.
- [21] T. Wauters *et al.*, “Wall conditioning in fusion devices with superconducting coils,” *Plasma Phys. Control. Fusion*, vol. 62, no. 3, Art. no. 3, Jan. 2020, doi: 10.1088/1361-6587/ab5ad0.
- [22] A. Gorjaev *et al.*, “Wall conditioning at the Wendelstein 7-X stellarator operating with a graphite divertor,” *Phys. Scr.*, vol. T171, p. 014063, Jan. 2020, doi: 10.1088/1402-4896/ab60fa.
- [23] T. Härtl, A. Drenik, M. Kircher, V. Rohde, F. Stelzer, and W. Zeidner, “Optimization of the ASDEX Upgrade glow discharge,” *Fusion Eng. Des.*, vol. 124, pp. 283–286, Nov. 2017, doi: 10.1016/j.fusengdes.2017.04.029.
- [24] F. L. Tabarés, D. Tafalla, and T. Wauters, “Plasma-Assisted Wall Conditioning of Fusion Devices: A Review,” in *Plasma Applications for Material Modification*, Jenny Stanford Publishing, 2021, p. 350.
- [25] D. Douai *et al.*, “Ion cyclotron wall conditioning in KSTAR and ASDEX-upgrade,” in *40th EPS Conference on Plasma Physics*, Finland, 2013, vol. P2.120.
- [26] M. Zlobinski, “LIDS,” *Phys. Scripta*, 2021.
- [27] D. Douai *et al.*, “Wall conditioning for ITER: Current experimental and modeling activities,” *J. Nucl. Mater.*, vol. 463, pp. 150–156, Aug. 2015, doi: 10.1016/j.jnucmat.2014.12.034.
- [28] T. Wauters *et al.*, “Isotope exchange by Ion Cyclotron Wall Conditioning on JET,” *J. Nucl. Mater.*, vol. 463, pp. 1104–1108, Aug. 2015, doi: 10.1016/j.jnucmat.2014.12.097.
- [29] A. Gorjaev *et al.*, “The upgraded TOMAS device: A toroidal plasma facility for wall conditioning, plasma production, and plasma–surface interaction studies,” *Rev. Sci. Instrum.*, vol. 92, no. 2, p. 023506, Feb. 2021, doi: 10.1063/5.0033229.
- [30] D. Kogut, D. Douai, G. Hagelaar, and R. A. Pitts, “Modelling of tokamak glow discharge cleaning II: comparison with experiment and application to ITER,” *Plasma Phys. Control. Fusion*, vol. 57, no. 2, Art. no. 2, Dec. 2014, doi: 10.1088/0741-3335/57/2/025009.
- [31] S. Moon *et al.*, “Characterization of neutral particle fluxes from ICWC and ECWC plasmas in the TOMAS facility,” *Phys. Scr.*, vol. 96, no. 12, p. 124025, Sep. 2021, doi: 10.1088/1402-4896/ac2494.
- [32] J. Gaspar, F. Rigollet, J.-L. Gardarein, C. Le Niliot, and Y. Corre, “In-situ estimation of the thermal resistance of carbon deposits in the JET tokamak,” *Int. J. Therm. Sci.*, vol. 104, pp. 292–303, Jun. 2016, doi: 10.1016/j.ijthermalsci.2016.01.022.